Gibberellic Acid-Induced Aleurone Layers Responding to Heat Shock or Tunicamycin Provide Insight into the *N*-Glycoproteome, Protein Secretion, and Endoplasmic Reticulum Stress[1][W]

Gregorio Barba-Espín, Plaipol Dedvisitsakul, Per Hägglund, Birte Svensson, and Christine Finnie*

Agricultural and Environmental Proteomics (G.B.-E., C.F.) and Enzyme and Protein Chemistry (P.D., P.H., B.S.), Department of Systems Biology, Technical University of Denmark, 2800 Kongens Lyngby, Denmark

The growing relevance of plants for the production of recombinant proteins makes understanding the secretory machinery, including the identification of glycosylation sites in secreted proteins, an important goal of plant proteomics. Barley (*Hordeum vulgare*) aleurone layers maintained in vitro respond to gibberellic acid by secreting an array of proteins and provide a unique system for the analysis of plant protein secretion. Perturbation of protein secretion in gibberellic acid-induced aleurone layers by two independent mechanisms, heat shock and tunicamycin treatment, demonstrated overlapping effects on both the intracellular and secreted proteomes. Proteins in a total of 22 and 178 two-dimensional gel spots changing in intensity in extracellular and intracellular fractions, respectively, were identified by mass spectrometry. Among these are proteins with key roles in protein processing and secretion, such as calreticulin, protein disulfide isomerase, proteasome subunits, and isopentenyl diphosphate isomerase. Sixteen heat shock proteins in 29 spots showed diverse responses to the treatments, with only a minority increasing in response to heat shock. The majority, all of which were small heat shock proteins, decreased in heat-shocked aleurone layers. Additionally, glycopeptide enrichment and *N*-glycosylation analysis identified 73 glycosylation sites in 65 aleurone layer proteins, with 53 of the glycoproteins found in extracellular fractions and 36 found in intracellular fractions. This represents major progress in characterization of the barley *N*-glycoproteome, since only four of these sites were previously described. Overall, these findings considerably advance knowledge of the plant protein secretion system in general and emphasize the versatility of the aleurone layer as a model system for studying plant protein secretion.

Plant proteins that are secreted to the apoplast have important functions in signaling, defense, and cell regulation. The classical protein secretory pathway is less characterized in plants than in mammals or yeast but is of growing interest due to the potential of plant systems as hosts for the production of recombinant proteins (Erlendsson et al., 2010; De Wilde et al., 2013). Plant secretomics, therefore, is a rapidly expanding area applied to gain further insight into these processes (Agrawal et al., 2010; Alexandersson et al., 2013). Many secretory proteins contain putative *N*-glycosylation sites, and the identification and characterization of these sites is an important element in secretomics analysis. However, to date, only a few plant glycoproteomes have been described (Fitchette et al., 2007; Minic et al., 2007; Palmisano et al., 2010; Melo-Braga et al., 2012; Zhang et al., 2012; Thannhauser et al., 2013).

The cereal aleurone layer is of major importance due to its central role in grain germination. Previous proteomic studies have been reported for aleurone layers dissected from mature (Finnie and Svensson, 2003) and germinating (Bønsager et al., 2007) barley (*Hordeum vulgare*) or developing (Tasleem-Tahir et al., 2011) and mature (Laubin et al., 2008; Jerkovic et al., 2010; Meziani et al., 2012) wheat (*Triticum aestivum*) grains. The in vitro culture of isolated aleurone layers was developed by Chrispeels and Varner (1967). Since then, this system has become an excellent tool for the study of germination signaling in response to phytohormones (Bush et al., 1986; Jones and Jacobsen, 1991; Bethke et al., 1997; Ishibashi et al., 2012). More recently, it has been adopted as a unique system for the analysis of plant secretory proteins (Hägglund et al., 2010; Finnie et al., 2011). The addition of GA_3 to the isolated aleurone layers induces the synthesis and secretion of hydrolytic enzymes. In the in vitro system, these accumulate in the incubation buffer, facilitating their identification and characterization using proteomics techniques. Thus, numerous secreted proteins with roles in the hydrolysis of starch, cell wall polysaccharides, and proteins could be identified (Finnie et al., 2011). Furthermore, several of the proteins were also detected in intracellular extracts from

[1] This work was supported by the Carlsberg Foundation (to B.S.), the Danish Council for Independent Research, Natural Sciences, the Centre for Advanced Food Studies, and the Thai Royal Government (Ph.D. stipend to P.D.).

* Address correspondence to csf@bio.dtu.dk.

The author responsible for distribution of materials integral to the findings presented in this article in accordance with the policy described in the Instructions for Authors (www.plantphysiol.org) is: Christine Finnie (csf@bio.dtu.dk).

[W] The online version of this article contains Web-only data.
www.plantphysiol.org/cgi/doi/10.1104/pp.113.233163

the same aleurone layers, presumably prior to their release. Many of the proteins appeared in multiple forms on two-dimensional (2D) gels, and often with higher M_r than expected, suggesting the presence of posttranslational modifications (PTMs; Finnie et al., 2011). Bak-Jensen et al. (2007) and Finnie et al. (2011) observed a highly complex pattern of α-amylase-containing spots on 2D gels, which originated from only two α-AMYLASE2 (AMY2) and two AMY1 gene products from a total of 10 genes, probably reflecting multiple forms due to PTMs.

In eukaryotic cells, proteins synthesized in the endoplasmic reticulum (ER) must be correctly folded and assembled before continuing in the secretory pathway. Perturbations of redox state, calcium regulation, Glc deprivation, and viral infection can lead to ER stress, triggered by the accumulation of unfolded and misfolded proteins in the ER lumen. This provokes a triple response from the cell, consisting of an up-regulation of chaperones and vesicle trafficking, a down-regulation of genes encoding secretory proteins, and an up-regulation of proteins involved in endoplasmic reticulum-associated protein degradation (ERAD). In plants, the molecular mechanisms underlying ER stress in plants have yet to be fully resolved (Martínez and Chrispeels, 2003; Nagashima et al., 2011; Moreno et al., 2012).

Tunicamycin (TN), an inhibitor of GlcNAc phosphotransferase, which catalyzes the first step in glycoprotein synthesis, has been used to induce ER stress by causing the accumulation of unfolded proteins in the ER lumen (Noh et al., 2003; Kamauchi et al., 2005; Reis et al., 2011). If unfolded proteins are not removed, the prolonged stress will induce programmed cell death. Links between ER stress and apoptosis have been reported in response to TN treatment in mammalian cells, whereas in plants, this correlation has been suggested, but the pathways of signal transduction remain unknown (Kamauchi et al., 2005; Reis et al., 2011).

In all plant tissues, heat shock (HS) induces the synthesis of a variety of heat shock proteins (HSPs), which are responsible for protein refolding under stress conditions (Craig et al., 1994) and translocation and degradation in a broad array of normal cellular processes (Bond and Schlesinger, 1986; Spiess et al., 1999). In the barley aleurone layer, HS selectively suppresses the synthesis of secretory proteins, including α-amylase, due to the selective destabilization of secretory protein mRNA (Belanger et al., 1986; Brodl and Ho, 1991). However, an acclimation effect has been described in aleurone cells after prolonged incubation at warm temperatures, resulting in a resumption of the protein secretory machinery (Shaw and Brodl, 2003). The connection between heat stress response and ER stress has been well established in mammals and yeast, but scarce information is available in plants (Denecke et al., 1995).

Over the last years, the dual role of reactive oxygen species (ROS) has been established in plants: at higher concentrations, ROS act as toxic molecules damaging cellular macromolecules, eventually causing cell death, but at lower concentrations, ROS seem to be necessary for seed germination and seedling growth by controlling the cellular redox status, regulating growth and protecting against pathogens (Bailly, 2004; Bailly et al., 2008). In the barley aleurone layer, GA_3 perceived at the plasma membrane induces ROS generation as a by-product from intense lipid metabolism, and the redox regulation of the GA_3-induced response has been proposed (Maya-Ampudia and Bernal-Lugo, 2006). This suggests that during the secretory function of the tissue, moderate levels of ROS may be acting as cellular messengers. In aleurone cells, ROS, especially hydrogen peroxide (H_2O_2), are involved in the process of programmed cell death, but the molecular mechanisms remain unclear (Bethke and Jones, 2001; Ishibashi et al., 2012).

Until now, none of the protein components of the ER stress pathways have been identified in barley; also, little is known about the glycosylation of barley proteins. In this work, numerous *N*-glycoslation sites are identified, and the effect of perturbing *N*-glycosylation and the secretory pathway by TN and HS treatments is analyzed in GA_3-induced barley aleurone layers.

RESULTS

The Effect of TN and HS on α-Amylase Production in GA_3-Induced Aleurone Layers

Since α-amylase is the most prominent secreted enzyme produced by aleurone cells in response to GA_3, a perturbation of the secretory machinery by TN or HS may affect the amount of this enzyme. Western blotting was used to detect α-amylase in the extracellular and intracellular fractions from aleurone layers incubated for 24 h. Untreated, GA_3-induced, and GA_3-induced aleurone layers in combination with HS or TN treatment were compared (Fig. 1). A decrease in α-amylase could be observed, both in the extracellular (Fig. 1A) and intracellular (Fig. 1B) fractions, when GA_3-induced cells were treated with 5 or 20 $\mu g\ mL^{-1}$ TN. Higher TN concentrations did not elicit a further decrease in the amount of α-amylase (data not shown).

For HS treatment, a temperature of 40°C was applied for the final 4 h of the 24-h incubation period. The HS treatment caused a decrease in α-amylase in the intracellular fraction (Fig. 1B) and in α-amylase secreted during the final 4 h when compared with GA_3-induced aleurone cells (Fig. 1A). Longer incubation periods at 40°C had no apparent effect on the amount of α-amylase (data not shown), most likely due to the acclimation response reported previously (Shaw and Brodl, 2003).

GA_3-Induced Cell Death Correlates with Enhanced H_2O_2 and Lipid Peroxidation

Both H_2O_2 content and thiobarbituric acid-reactive substances (TBARS) indicating lipid peroxidation were increased in extracts from GA_3-induced aleurone layers in comparison with untreated samples (Fig. 2A). Treatment of GA_3-induced aleurone layers with 5 $\mu g\ mL^{-1}$ TN or with HS did not result in further increases, but

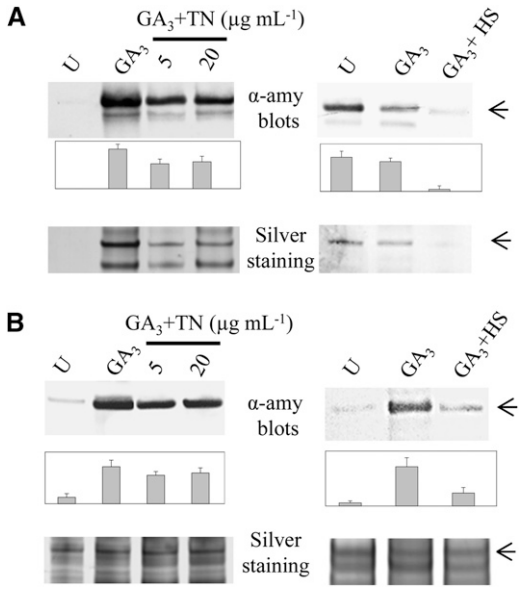

Figure 1. Western blots probing α-amylase in the extracellular (A) and intracellular (B) water-soluble protein fractions of in vitro-incubated aleurone layers. Equal volumes of extracellular protein fraction (A) and equal amounts of total protein (B) were applied to SDS-PAGE. For each blot, a parallel protein gel was stained with silver nitrate. Bands corresponding to the α-amylase (45 kD) are indicated by arrowheads. Densitometric quantification of western-blot signals was performed using ImageJ software (National Institutes of Health) and is expressed as the average of three biological replicates plus SE (bar charts). HS, 4-h HS; U, untreated.

20 μg mL^{-1} TN significantly enhanced the level of lipid peroxidation.

In order to examine whether TN and HS could affect the viability of barley cells, cell death was monitored and quantified in intact aleurone layers by simultaneous staining of live and dead cells with fluorescent probes (Fig. 2B). The cell death quantitation reflected a correlation with the endogenous H_2O_2 and lipid peroxidation measurements. GA_3 treatment of barley aleurone cells resulted in increased cell death, while untreated aleurones maintained higher cell viability. Hence, after 24 h of incubation, 45% of GA_3-induced cells were dead, whereas 81% of untreated cells remained alive (Fig. 2B). GA_3 + HS and GA_3 + 5 μg mL^{-1} TN did not result in increased cell death, whereas cell death was enhanced in GA_3 + 20 μg mL^{-1} TN samples (Fig. 2B). Treatments of GA_3-induced aleurone layers with 5 μg mL^{-1} TN and 4 h of HS were selected for comparative proteome analysis, since these affected protein secretion without provoking massive oxidative damage and cell death.

Fluorescent Glycoprotein Staining and Protein Identification

To visualize glycoproteins and assess the effect of TN treatment on protein glycosylation, extracellular proteins from GA_3-induced and GA_3 + 5 μg mL^{-1} TN-treated aleurone layers were resolved by 2D SDS-PAGE, and the glycoproteins were detected by Pro-Q Emerald staining. As expected, TN greatly reduced the glycosylation of extracellular proteins (Fig. 3A). The fact that some highly abundant proteins did not react with the Pro-Q Emerald stain whereas some low-abundance proteins reacted strongly supports the specificity of Pro-Q Emerald staining for glycoproteins. To reduce the risk of false positives, of the 53 fluorescent spots visible in all three GA_3-treated replicates, only the 23 intense spots missing after TN treatment (numbered spots in Fig. 3B) were analyzed by mass spectrometry. Proteins were identified in 14 spots (Supplemental Table S1). Sequence analysis (http://www.cbs.dtu.dk/services/NetNGlyc/) confirmed the presence of at least one putative *N*-glycosylation site in each identified protein (data not shown).

Proteome Analysis of the Extracellular Fraction from in Vitro Incubated Aleurone Layers

2D gel electrophoresis (pH 3→10) was used to profile the extracellular protein fraction from the four aleurone layer treatments. Clear differences were apparent between 2D gel electrophoresis patterns of untreated and GA_3-induced aleurone layers as well as between GA_3-induced aleurone layers and each stress treatment (Fig. 4A). In total, the average volumes of 35 spots varied by at least 1.5-fold among the four treatments. These spots were chosen for further analysis, and 22 were identified

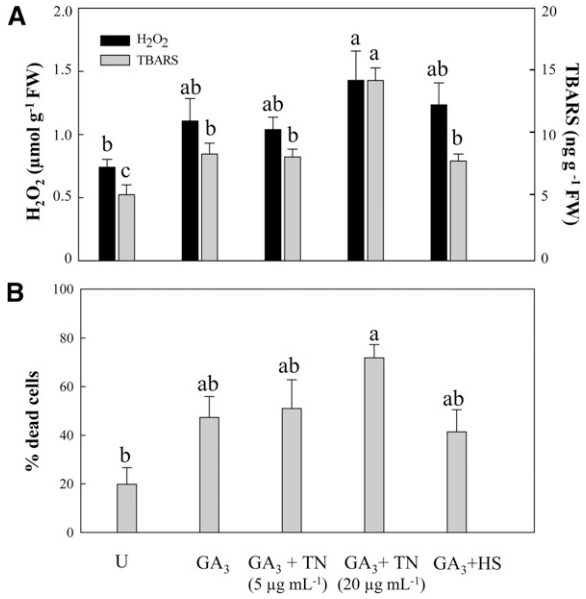

Figure 2. Enhanced cell death in GA_3-induced aleurone layers correlates with higher endogenous H_2O_2 and lipid peroxidation contents. A, H_2O_2 and TBARS were measured in aleurone layer extracts. B, Vital staining was performed in intact aleurone layers, and randomly selected fields were counted to determine the percentage of dead cells. Different letters indicate statistical significance according to Tukey's test ($P < 0.05$). FW, Fresh weight; U, untreated.

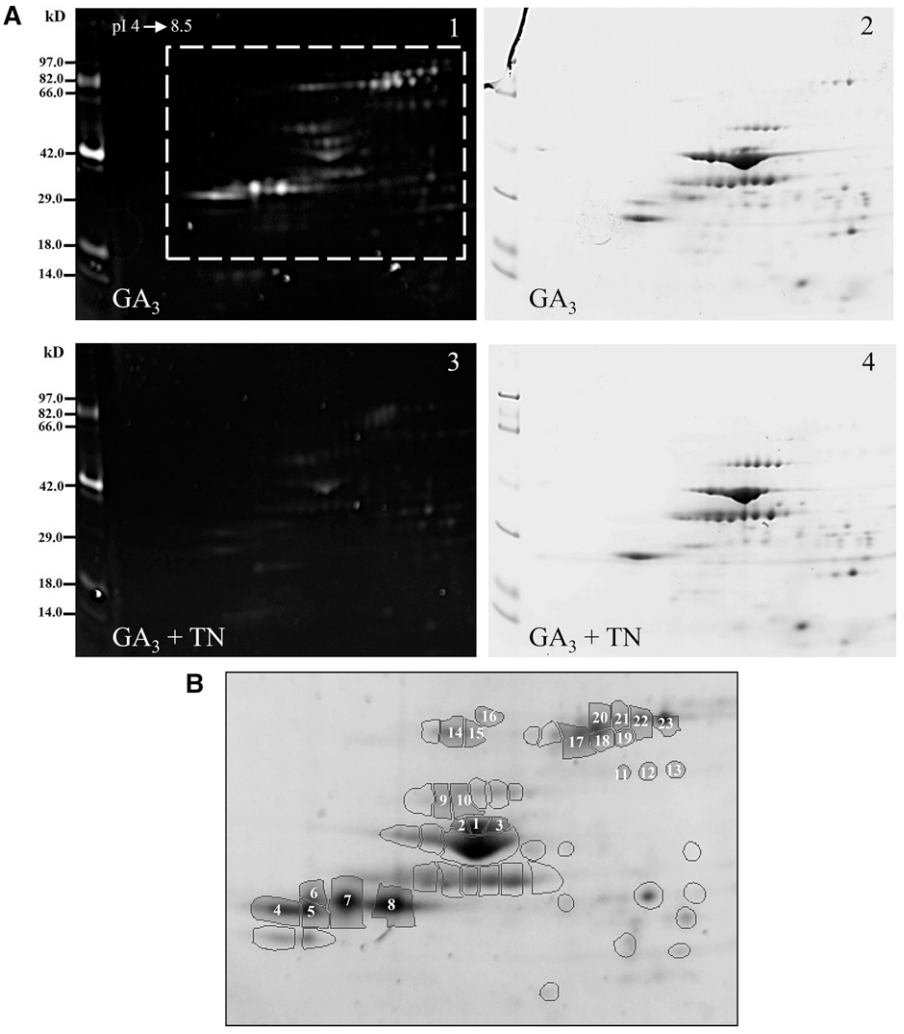

Figure 3. Fluorescent glycoprotein staining of extracellular proteins. A, One representative glycoprotein-stained gel (gels 1 and 3) and a corresponding colloidal Coomassie blue-stained gel (gels 2 and 4) covering the pH range 4 to 8.5 are shown for GA_3-induced (gels 1 and 2) and GA_3 + 5 μg mL^{-1} TN-treated (gels 3 and 4) aleurone layers. Molecular size markers are indicated at left. B, View of the GA_3 reference gel framed in A showing 53 intense fluorescent spots present in all GA_3 replicates. Twenty-three of them (numbered spots) correspond to spots absent in GA_3 + TN aleurone layers, of which 14 were identified by mass spectrometry. (For details about protein identifications, see Supplemental Table S1).

by mass spectrometry (Fig. 4B; Supplemental Table S2). As expected, most of them were α-amylases and proteases (Fig. 4C). The spots formed three clusters according to their appearance profiles (Fig. 5). Protein spots in cluster A (13 spots) increased in response to GA_3, 11 contained α-amylases (AMY1 and AMY2) and one contained a Cys proteinase (EP-B1). Moreover, four spots decreased in GA_3 + TN samples (cluster B). Here, one AMY2 spot migrated more slowly than the other identified AMY1 and AMY2 spots (Supplemental Table S2), indicating that this upper spot may be glycosylated. Finally, five spots decreased in intensity in both treatments (cluster C). Cluster C contains four protease spots (two Cys proteinase and two cathepsin) with higher experimental M_r than Cys proteinase spots in clusters A and B, again suggesting the presence of PTMs (Supplemental Table S2).

Proteome Analysis of Aleurone Layer Intracellular Extracts

Intracellular water-soluble proteins from the four samples described above were also analyzed using 2D gel electrophoresis (Fig. 6A) and mass spectrometry. The image analysis showed 250 protein spots varying among the four treatments (Fig. 6B). Of these, 178 were identified (Fig. 6B; Supplemental Table S3) and assigned to seven functional categories (Fig. 6C). Among the identified proteins, 55% (98 protein spots) are involved in primary metabolism; the remaining proteins were functionally assigned as chaperones (29), polysaccharide hydrolases (11), detoxification enzymes (12), signaling proteins (nine), and defense proteins (four), and a considerable number of identified spots (16) were proteins of unknown function (Fig. 6C). Principal component analysis (PCA) performed on these differentially changed spots (Fig. 7A) indicated the presence of six clusters based on similarity of expression profiles (Fig. 7B). Proteins in cluster A (decreased in GA_3 and GA_3 + TN aleurone samples and increased in GA_3 + HS samples) and in cluster B (increased in GA_3 + HS samples) were mainly proteins involved in primary metabolism, such as glycolysis, citric acid cycle, and amino acid biosynthesis. Remarkably, 11 out of 22 spots in cluster C with lower abundance in GA_3 + HS samples contain small HSPs. In cluster D, the spots from the three samples incubated

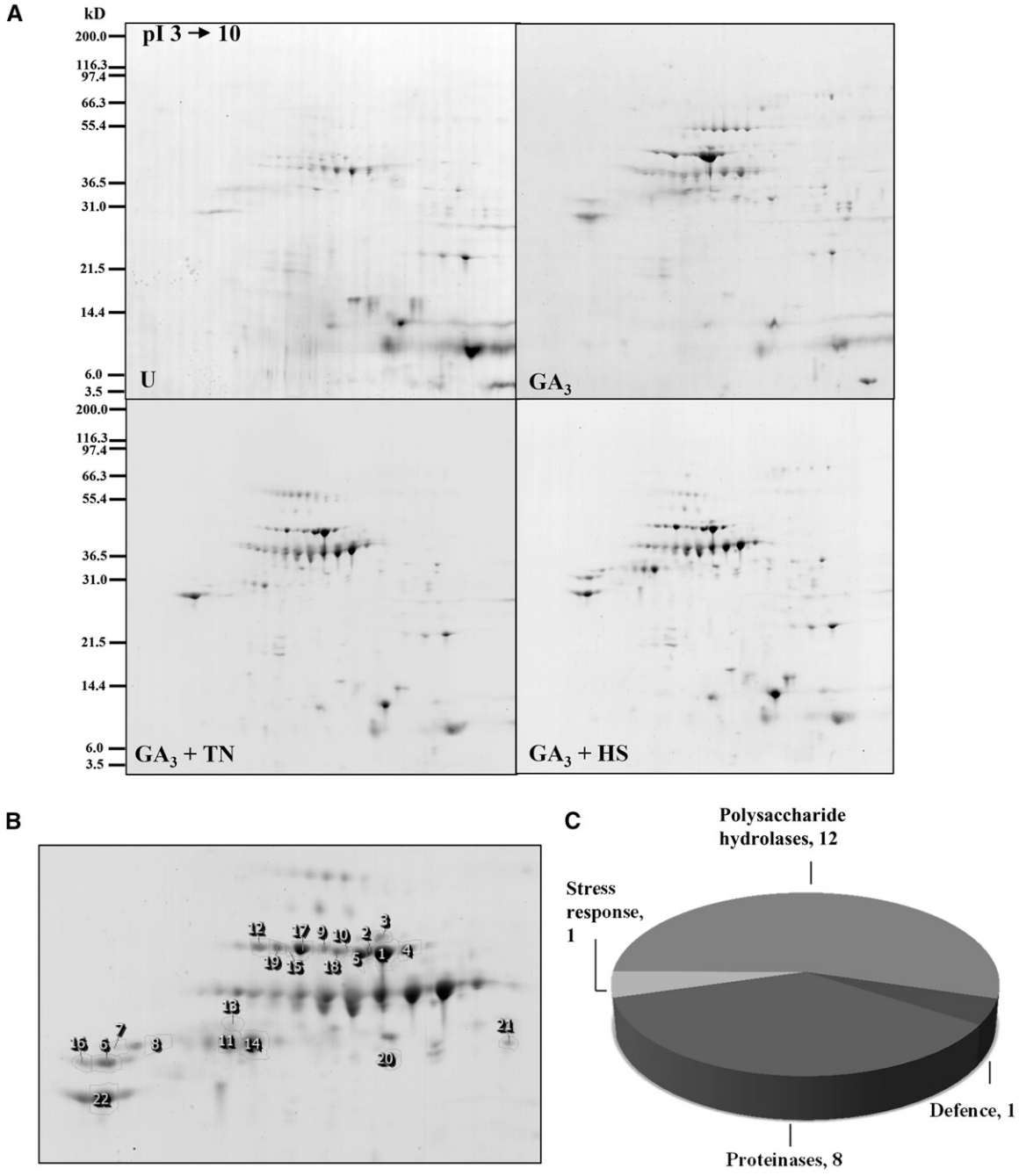

Figure 4. Extracellular protein profiles of barley aleurone layer extracts. A, One representative colloidal Coomassie blue-stained gel covering the pH range 3 to 10 is shown for each treatment. Molecular size markers are indicated at left. U, Untreated. B, Closeup view of the reference gel showing 22 identified spots. C, Functional categories of the plant proteins identified. (For details about protein identifications, see Supplemental Table S2).

with GA_3 decreased in volume when compared with untreated samples; it is also very interesting that 38% of the identifications in cluster D were proteins of unknown function. Clusters C and E grouped protein spots whose profiles dramatically decreased in HS samples when compared with GA_3- and GA_3 + TN-treated samples. Proteins in 28 spots in cluster E belong to primary metabolism, indicating heat-induced protein degradation; remarkably, three AMY1 and three AMY2 spots were assigned to cluster E, suggesting selective destabilization of secretory protein mRNA by heat stress. Finally, spots showing increases both in GA_3 + TN and GA_3 + HS samples were grouped in the small cluster F, including several late embryogenesis abundant

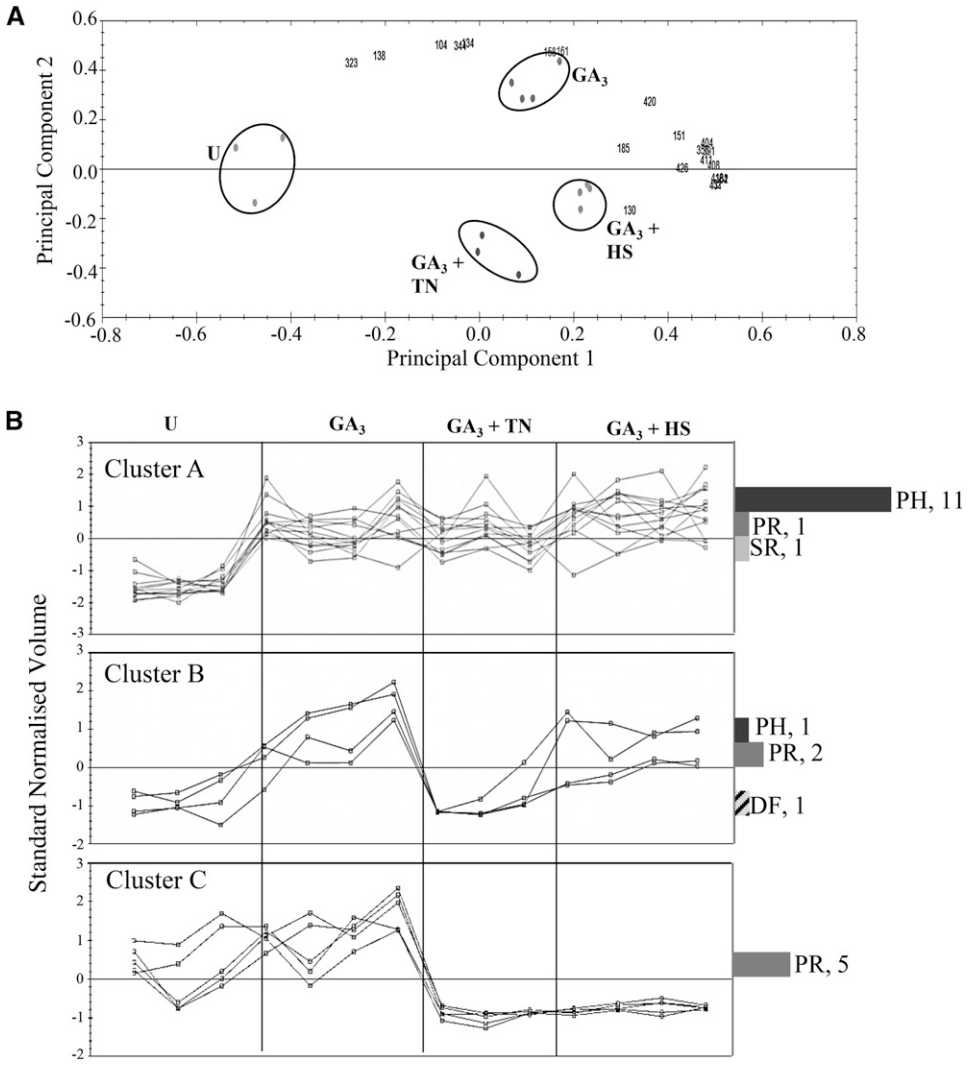

Figure 5. PCA and clustering of extracellular protein spots. A, PCA was performed on the 22 identified spots. Biological replicates are grouped by circles, and spots are indicated by numbers. B, Expression profiles of protein spots from PCA analysis were grouped in three clusters. The normalized volume for each spot is expressed relative to a reference gel (GA_3), in which all spot volumes are by default set to 1. Corresponding functional classifications are indicated: DF, defense; PH, polysaccharide hydrolase; PR, protease; SR, stress response. U, Untreated. (For details about protein identifications, see Supplemental Table S2).

proteins and protein disulfide isomerase (PDI). Furthermore, among the six clusters there were 19 protein spots suspected to be protein fragments due to a clear discordance between theoretical and experimental pI and M_r (Supplemental Table S3). In accordance with this, their sequence coverages obtained by Mascot search were confined to the N- or C-terminal parts of the protein. Curiously, 17 of these 19 protein fragments belong to cluster E.

Identification of *N*-Glycosylated Proteins from Complex Protein Samples

An *N*-glycoproteome analysis was performed in both intracellular and extracellular fractions from aleurone layers in order to provide the first overview of glycosylation sites in barley proteomes. Enrichment of glycopeptides from trypsin-digested protein extracts was carried out by hydrophilic interaction liquid chromatography (HILIC), followed by deglycosylation using PNGase A in the presence of $H_2{}^{18}O$. During the deglycosylation reaction, the formerly glycosylated Asn residues undergo deamidation and ^{18}O is incorporated into the carboxylate groups of the resulting Asp side chains. Deglycosylated Asn residues can thus be distinguished from residues that were deamidated prior to the PNGase A reaction. Analysis by liquid chromatography (LC)-tandem mass spectrometry (MS/MS) on a Q-Exactive Orbitrap enabled the determination of 73 independent glycopeptides in 65 glycoproteins (Table I; Supplemental Table S4). Of these, 57 glycoproteins were found in the extracellular fraction, whereas 36 glycoproteins were identified in the intracellular samples. A total of 28 proteins were found in both fractions. All the glycoproteins were predicted to follow the secretory pathway according to the signal peptide cleavage site prediction (Supplemental Table S4).

DISCUSSION

By the application of two stresses that affect protein secretion through independent mechanisms, new

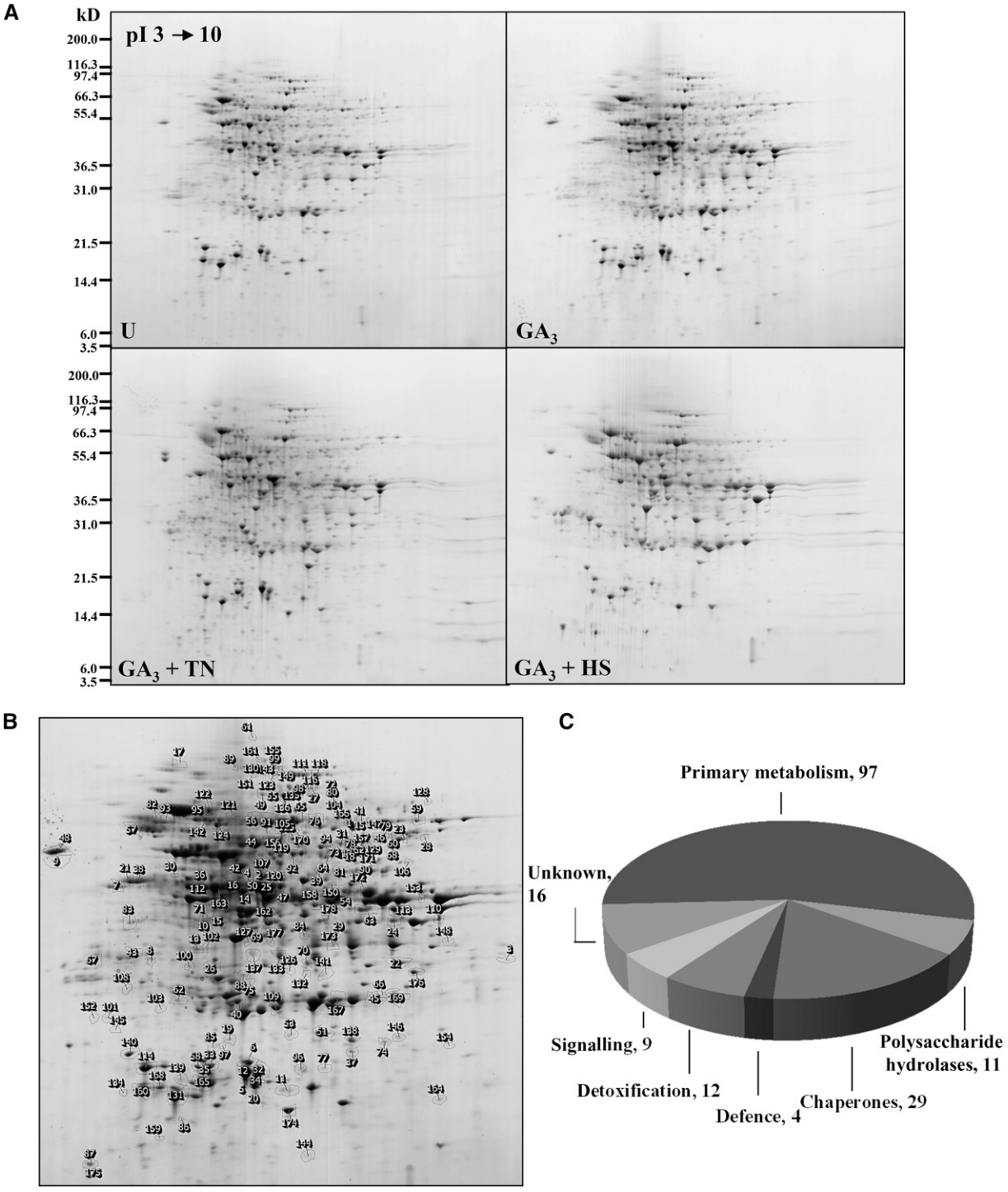

Figure 6. Intracellular water-soluble protein profiles of barley aleurone layer extracts. A, One representative colloidal Coomassie blue-stained gel covering the pH range 3 to 10 is shown for each treatment. Molecular size markers are indicated at left. U, Untreated. B, Closeup view of the reference gel showing 178 identified spots. C, Functional categories of the plant proteins identified. (For details about protein identifications, see Supplemental Table S3).

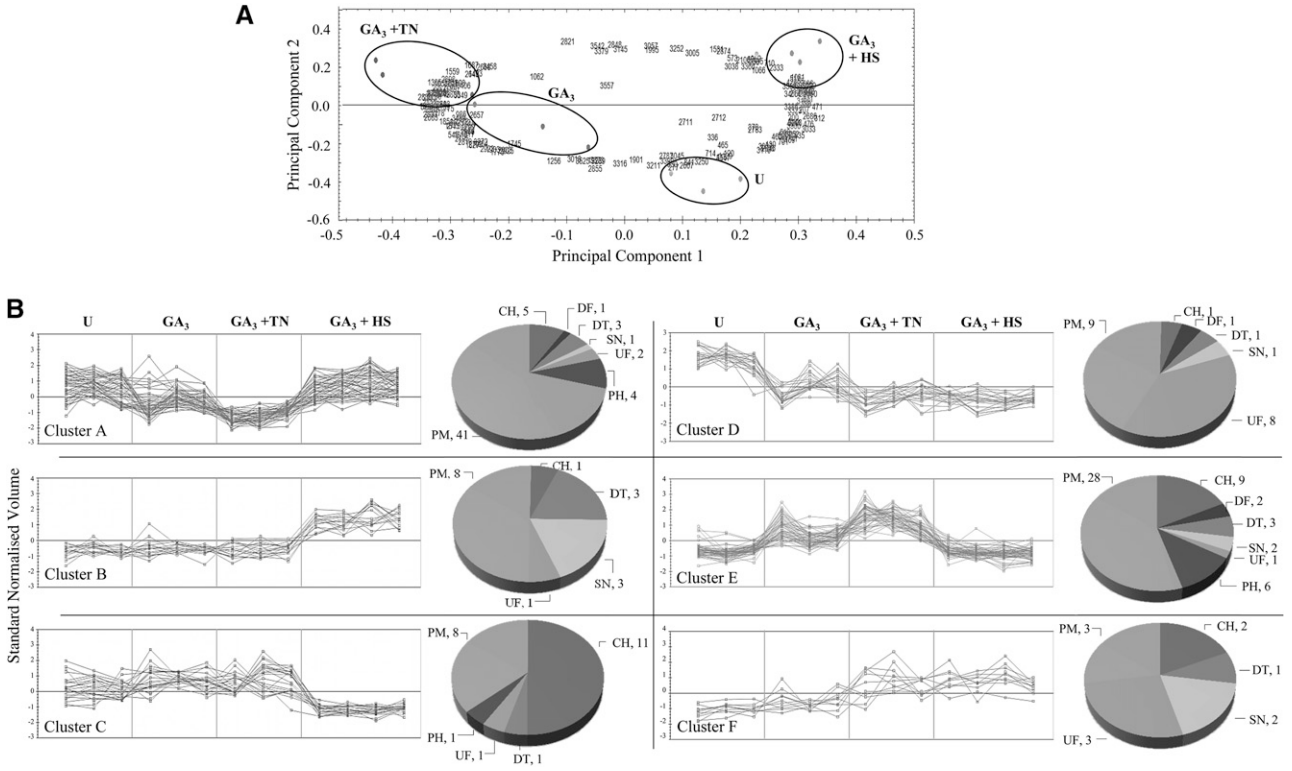

Figure 7. PCA and clustering of intracellular water-soluble protein spots. A, PCA was performed on the 178 identified spots. Biological replicates are grouped by circles, and spots are indicated by numbers. B, Expression profiles of protein spots from PCA analysis were grouped in six clusters. The normalized volume for each spot is expressed relative to a reference gel (GA_3), in which all spot volumes are by default set to 1. Corresponding functional classifications are indicated: CH, Chaperone; DF, defense; DT, detoxification enzymes; PH, polysaccharide hydrolase; PM, primary metabolism; SN, signaling; UF, unknown function. U, Untreated. (For details about protein identifications, see Supplemental Table S3).

information about the plant protein secretion system in GA_3-induced aleurone layers has been obtained.

A clear effect of GA_3 on H_2O_2 production and cell death was confirmed (Bethke and Jones, 2001; Ishibashi et al., 2012). Moreover, lipid peroxidation, as indicative of cell damage in response to several stresses (Bailly, 2004; Barba-Espín et al., 2011), was enhanced by GA_3 (Fig. 2A). A high TN concentration (20 μg mL^{-1}) provoked further H_2O_2 accumulation and cell death, which is probably due to the oxidative damage enhanced in these samples. The inhibition of protein folding and blocking of secretion provoked by high TN concentrations seemed to be incompatible with cellular function, whereas the response triggered by lower TN concentrations may still allow recovery of the ER function.

Overall, GA_3 induced protein secretion from aleurone layers as shown (Finnie et al., 2011). Half of the observed spots decreased in abundance under one or both of the stress treatments. Most of these contained proteases, whereas the majority of the α-amylase spots remained at similar levels to unstressed (GA_3-induced) aleurone layers (Figs. 4 and 5; Supplemental Table S2). Cys proteinases are the most abundant proteases secreted by barley aleurone layers in response to GA_3 (Zhang and Jones, 1995; Martinez and Diaz, 2008), and the synthesis of several family members remains high during the first 36 h of GA_3 incubation (Koehler and Ho, 1990). By contrast, α-amylase secretion peaks much earlier during the first 24 h of incubation (Bethke et al., 1997). Thus, the difference in the responses of proteases and α-amylase to the treatments could be due to more significant secretion of Cys proteases than α-amylases during the 4-h period of HS.

In the intracellular proteomes, 178 spots changed abundances and were assigned to six clusters (Figs. 6 and 7). The overall effect of TN and HS treatments on the intracellular spot patterns reflects a differential protein response; HS provoked major changes in the protein patterns when compared with treatments with GA_3 alone and TN, as expected due to the suppression of secretory protein synthesis (Brodl and Ho, 1991; Spiess et al., 1999) and the more selective mechanism of the TN effect on the ER lumen. Considering the short incubation time at 40°C, the major changes occurring in HS samples suggest changes in protein turnover. In fact, the most dramatic variations between GA_3 and stress treatments correspond to spots either decreasing or increasing in HS samples (Fig. 7; Supplemental

Table I. *A total of 65 N-glycoproteins was identified from extracellular and intracellular complex samples*

Independent glycopeptides identified by LC-MS/MS analysis are shown in parentheses after the accession numbers. For details about protein identifications, see Supplemental Table S4.

Protein Name	Accession No.	Protein Name	Accession No.
Acidic endochitinase	MLOC_72826.1 (1)	Lipid transfer proteins	AK369929 (1)
α-Galactosidase	AK364576 (1)		AK367409 (1)
α-Glucosidase	MLOC_66806.2 (2)	Lysosomal α-mannosidase	AK364106 (2)
Amino oxidase	AK353856 (1)	MtN19-like protein	MLOC_73878.1 (2)
Aminoacylase1	AK376199 (1)	Pectin lyase-like superfamily	MLOC_75889.3 (1)
	MLOC_64721.1 (1)	Pectinesterase	AK366148 (1)
Aminopeptidase M1	AK358827 (1)	Peptidyl-prolyl cis-trans-isomerase	MLOC_38535.3 (1)
Arabinofuranosidases A	MLOC_44256.2 (1)	Peroxidase	MLOC_56862.1 (1)
	MLOC_56099.3 (1)	Phospholipase C-like phosphodiesterase	MLOC_65228.1 (1)
Aspartic protease family proteins	AK376209 (1)	PDI	AK370108 (1)
	MLOC_13635.1 (1)	Purple acid phosphatases	AK360979 (1)
Auxin-induced-like protein	MLOC_57260.1 (1)		AK354837 (1)
β-D-Xylosidase	MLOC_62475.1 (1)		MLOC_34761.1 (1)
β-Fructofuranosidase	AK252358.1 (1)	Receptor-like protein kinases	AK364371 (1)
β-Galactosidase	AK252929.1 (1)		MLOC_53309.2 (2)
β-Glucosidase-like hydrolase	AK374484 (1)	Secretory peroxidases	AK365489 (1)
Calreticulin	MLOC_67890.1 (1)		MLOC_72727.1 (1)
Cathepsin F-like Cys protease	MLOC_61862.1 (1)	Ser carboxypeptidases	AK365716 (1)
Chitinase	AK376513 (1)		MLOC_55542.1 (2)
Early nodulin-like protein3	MLOC_4663.1 (1)		AK372814 (1)
Endonuclease	MLOC_5210.1 (1)		AK362092 (1)
Epidermal growth factor-like	AK370029 (1)	Subtilisin-like protease	MLOC_64136.1 (1)
Glycerophosphoryl diester phosphodiesterase	AK248297.1 (2)	Thioredoxin-like protein	AK359722 (2)
GDSL-motif esterase/lipases	MLOC_75385.1 (1)	Transmembrane9 family protein	MLOC_11918.1 (1)
	MLOC_12361.1 (1)	UDP-Glc 4-epimerase	MLOC_60662.1 (1)
Globulin3	MLOC_59994.1 (1)	Unannotated protein	MLOC_5243.1 (1)
Glucan 1,3-β-glucosidase	AK376623 (1)		MLOC_10934.1 (1)
Glutamyl-tRNA amidotransferase	MLOC_60550.3 (1)	Vacuolar sorting receptor	AK248808.1 (1)
GPI-anchored protein2	MLOC_57195.1 (1)	Vicilin-like antimicrobial peptide	MLOC_57363.1 (1)
Indole-3-acetic acid-amino acid hydrolase ILR1	AK368695 (1)	Xylanase inhibitors	AK366716 (1)
Kinase, putative	MLOC_34836.3 (1)		MLOC_26558.1 (1)
Lectin-domain receptor-like kinase	MLOC_58449.1 (1)	Xyl isomerase	MLOC_55107.1 (1)
Leu-rich receptor kinase	MLOC_1088.10 (1)		

Table S3). Complementary expression profiles are observed for clusters A and E (Fig. 7), reflected by several full-length proteins in cluster A (aconitate hydratase, HSP70, enolase, aldose reductase, 6-phosphogluconate dehydrogenase, phospho*enol*pyruvate carboxylase, and malic enzyme) being present in cluster E as probable fragments.

The aleurone layer contains large reserves of oil, and GA_3 stimulates both fatty acid β-oxidation and the glyoxylate cycle for the production of Suc from storage lipids and to produce carbon skeletons for the production of secreted hydrolases (Doig et al., 1975; Eastmond and Jones, 2005). The glyoxylate cycle enzymes isocitrate lyase and aconitate hydratase were identified in 12 and eight spots, respectively, with a number of these containing fragments (Supplemental Table S3). Those migrating according to their predicted M_r and pI all decreased in intensity in GA_3 + TN samples, as did a predicted acyl-CoA oxidase identified in one spot (Supplemental Table S3). This suggests a down-regulation of β-oxidation and the glyoxylate cycle coupled to the decrease in production of secretory proteins.

In agreement with previous work (Finnie et al., 2011), several secretory proteins (AMY1 and AMY2, α-*N*-arabinofuranosidase A, β-D-xylosidase, and Ser carboxypeptidase) could be identified in intracellular aleurone layer extracts (Supplemental Table S3). These intracellular forms are presumably en route in the protein secretion pathway. Spots containing AMY1 and AMY2, α-*N*-arabinofuranosidase A, and β-D-xylosidase were decreased in the intracellular extracts subjected to TN or HS treatments. This decrease was not seen in the extracellular protein fractions (Fig. 4; Supplemental Table S2), probably reflecting that the secretory proteins are transiently present within the aleurone layers, while the extracellular fraction contains proteins accumulating over the entire incubation period. For this reason, it was not possible to observe a decrease in α-amylase after 4 h of HS by western blotting of extracellular proteins accumulated over 24 h (data not shown), although the decrease was apparent both in the intracellular fraction (Fig. 1B) and in the extracellular fraction collected solely during the 4-h period of HS (Fig. 1A).

Many of the extracellular and intracellular proteins (Supplemental Tables S2 and S3) migrated on gels with higher M_r than predicted, suggesting the presence of PTMs. These proteins were confirmed to have a leader peptide-processing site and at least one putative *N*-glycosylation site (data not shown). Information about the PTMs of barley α-amylases is lacking, but extensive modifications are suggested by the complex pattern of spots detected in both supernatant and intracellular fractions (Bak-Jensen et al., 2007; Finnie et al., 2011).

According to Swiss-Prot database predictions, more than 50% of eukaryotic proteins are glycosylated (Apweiler et al., 1999), the majority of them being related to the secretory system. Therefore, a large number of proteins are potential targets for TN action. Many studies have characterized a high number of glycoproteins from bacterial (Nothaft and Szymanski, 2010) and animal (Bunkenborg et al., 2004; Wollscheid et al., 2009; Zielinska et al., 2010) species. This work represents a major contribution toward mapping the barley glycoproteome, assigning 73 *N*-glycosylation sites in 65 proteins (Table I; Supplemental Table S4), several of which were found by 2D-based analysis either to increase (PDI and calreticulin) or decrease (β-xylosidase, α-*N*-arabinofuranosidase A, and Ser carboxypeptidase) in response to TN or HS treatments (Fig. 7; Supplemental Table S3). According to Uni-Prot database annotations, from the 65 assigned glycoproteins, only β-xylosidase, Ser carboxypeptidase, xylanase inhibitor, and oxalate oxidase were previously confirmed to be *N*-glycosylated in barley.

TN treatment of GA_3-induced aleurone layers resulted in a decrease in Pro-Q Emerald-stained glycoproteins in the extracellular fraction, including cathepsin B, Cys proteinase C1A, two α-amylase (AMY2), two purple acid phosphatase, two subtilisin-like Ser protease, and six β-glucosidase spots (Fig. 3; Supplemental Table S1). Of these, a corresponding glycopeptide was identified in a Cys proteinase, purple acid phosphatase, subtilisin-like Ser protease, and a β-glucosidase (Supplemental Table S4).

To date, no α-amylase form has been confirmed to be glycosylated. The barley seed complex 2D spot pattern obtained from a limited number of gene products (Bak-Jensen et al., 2007; Finnie et al., 2011) probably reflects PTMs. Here, we show by specific fluorescent staining that two AMY2 spots contain glycoproteins. In agreement with this, both forms migrated with an apparent molecular mass 2 kD larger than the theoretical value. Moreover, in GA_3-induced aleurone layers treated with TN, the corresponding AMY2 spots with elevated M_r decreased in intensity for both extracellular and intracellular fractions, representing the most significant intensity change in response to TN. By contrast, AMY2 forms migrating according to their predicted M_r were not affected by TN. A single *N*-glycosylation site is predicted in this AMY2 gene product; however, a corresponding glycopeptide was not identified. This may be due to the high hydrophilicity of this particular glycopeptide, hindering its retention on the reverse-phase column prior to mass spectrometry analysis. The glycosylated AMY2 forms identified here constitute a minor proportion of the total α-amylase produced by the isolated aleurone layers (Fig. 3) or in germinating grains (Bak-Jensen et al., 2007). Interestingly, the presence of glycosylated AMY2 varies among barley cultivars, since the AMY2 form with elevated M_r was only seen in some cultivars (Bak-Jensen et al., 2007). It remains to be determined whether the glycosylation affects the thermostability or kinetic properties of barley AMY2, as suggested for rice (*Oryza sativa*) Amy1A (Terashima et al., 1994).

Plant cells seem to have a common strategy for overcoming ER stress through (1) attenuation of genes encoding secretory proteins, (2) enhancement of protein-folding activity by chaperones, such as the ER-localized calreticulin or PDI, and (3) degradation of unfolded proteins by means of the ERAD system (Travers et al., 2000; Martínez and Chrispeels, 2003; Kamauchi et al., 2005). This study reveals components and evidence of this triple response. Five major HSP families are conserved among species (Wang et al., 2004): HSP60, HSP70, HSP90, HSP100, and small HSP (12–40 kD). Marked differences in proteins with chaperone functions were observed between TN and HS samples, suggesting different pathways in the induction of HSPs and the ER stress response (Johnston et al., 2007). Whereas TN treatment increased nine HSP spots (17, 26, and 70 kD), HS induced an increase in six HSP spots (17, 60, and 70 kD) but a decrease in 17 HSP spots (mainly small HSP). Thermoprotection in the aleurone has been reported to correlate more with enhanced levels of fatty acid saturation in membrane phospholipids than with HSP expression, since HSP70 synthesis was only slightly induced by 3 h of incubation at 40°C (Shaw and Brodl, 2003). Our results suggest an overall decrease of small HSP and an increase in certain intermediate- and high-M_r chaperones in HS samples; these observations indicate the differential HSP expression under HS and highlight the secondary role of HSPs in acquiring thermotolerance in barley aleurone cells. Moreover, five spots corresponding to HSP70 fragments decreased intensity in HS samples. In fact, some other metabolic protein spots judged to be the result of proteolytic processing were decreased after HS treatment, suggesting changes in protein turnover (Fig. 7; Supplemental Table S3).

Two important ER stress-induced chaperones were found to increase in response to both TN and HS treatments: calreticulin and PDI. Family members of these ER-resident multifunctional proteins are known to be specifically activated by *INOSITOL-REQUIRING ENZYME1/basic Leucine Zipper60* (*IRE1/bZIP60*) transcription factor, which is a mediator of the ER stress response (Ye et al., 2011; Moreno et al., 2012). Calreticulin was identified in two spots with the same pI on 2D gels but differing in molecular mass by about 2 kD, suggesting that the protein in the slower migrating

spot may be *N*-glycosylated and that in the faster migrating spot may be a nonglycosylated form. In agreement with this hypothesis, TN caused a specific increase in intensity of the lower spot, which was the most pronounced accumulation observed in response to TN, whereas the intensity of the upper spot decreased in abundance. By contrast, HS slightly reduced the level of the lower calreticulin spot and increased the upper spot (Supplemental Table S3). Thus, HS and TN have contrasting effects on the two calreticulin-containing spots. Moreover, PDI was identified in one spot increasing upon both TN and HS treatments (Supplemental Table S3). Glycosylation of both calreticulin and PDI was confirmed by identification of the predicted glycosylation site (Supplemental Table S4). Interestingly, the glycopeptides were identified in the extracellular fraction. The significance of this is unclear; however, calreticulin is known to have multiple cellular locations and in mammalian cells has been identified at the cell surface (Gardai et al., 2005; Gold et al., 2010). A further approach to gain insight on the biological role of calreticulin glycosylation is needed, but an effect on its interaction with other proteins and subcellular localization is expected. Two proteasome subunit spots were also induced, one of them upon TN treatment and the other after HS, both likely associated with the ERAD system.

Two 1-Cys peroxiredoxin spots differing in pI were identified (Supplemental Table S3). Besides its antioxidant role during barley germination (Stacy et al., 1999), a chaperone activity was demonstrated for 1-Cys peroxiredoxin from Chinese cabbage (*Brassica campestris* ssp. *pekinensis*) seeds (Kim et al., 2011). 1-Cys peroxiredoxins are susceptible to overoxidation of the active-site Cys, which can be observed in 2D gel electrophoresis, since this causes a pI shift of the protein (Pulido et al., 2009). Chaperone activity was increased in the overoxidized form, whereas the reduced form had greater peroxidase activity (Kim et al., 2011). In our experiments, these reduced and oxidized forms likely correspond to the high- and low-pI spots, respectively. HS and to a lesser extent TN treatment caused an increase in the reduced form and a decrease in the oxidized form, which might indicate a decrease in its chaperone activity and an enhanced antioxidant activity.

Cluster F (Supplemental Table S3) contained proteins in addition to PDI that increased in response to both stress treatments and, therefore, are strong candidates for having roles in ER stress mechanisms. Some of these are known to respond to various abiotic stresses, such as Glc and ribitol dehydrogenase (Witzel et al., 2010) and glyoxalase (Wu et al., 2013). Interestingly, a Rib-phosphate pyrophosphokinase (phosphoribosyl pyrophosphate synthase) was identified, which synthesizes phosphoribosyl pyrophosphate, an important intermediate in purine and pyrimidine biosynthesis (Zrenner et al., 2006) The increase in the amount of this protein could suggest a need for DNA repair. A putative isopentenyl diphosphate isomerase was also identified in this cluster (Supplemental Table S3). This enzyme belongs to the mevalonate pathway and is required for the synthesis of the polyisoprenoid lipid carrier for the glycans used in *N*-glycosylation (Jones et al., 2009). Therefore, a compensatory mechanism to restore the folding capacity of the ER might be suggested, although further approaches will be required to analyze the mevalonate pathway activity under stress conditions.

Notably, numerous proteins induced by TN treatment, including small HSPs and calreticulin (Supplemental Table S3), were also slightly up-regulated in GA_3-induced compared with untreated aleurone layers. This was reflected in the PCA, where grouping of the GA_3-induced and GA_3 + TN-treated aleurone layers suggested similar changes in comparison with the untreated samples, in contrast to the GA_3 + HS-treated aleurone layers (Fig. 7A). This suggests that the GA_3-induced aleurone layers may display early symptoms of ER stress due to the heavy load on the protein secretory machinery (Fig. 8). The experimental conditions used here were carefully chosen to avoid the induction of cell death due to ER stress but to inflict a subtle pressure on the protein secretory system. Further investigations along these lines of evidence will explore possible links between GA_3-induced cell death and ER stress in barley aleurone layers.

CONCLUSION

Overall, the data presented here provide new insights into the proteomes of in vitro maintained aleurone layers. (1) A large number of proteins have been identified in the intracellular water-soluble fraction, many of which had previously not been identified in barley aleurone layers. (2) We provide, to our knowledge, the first comparative study of the distinct and overlapping effects of TN and HS on a plant proteome and show that this strategy identifies key components of the protein secretory and quality-control machinery and also identifies proteins with likely functions in ER stress responses. In summary, HS entails a major

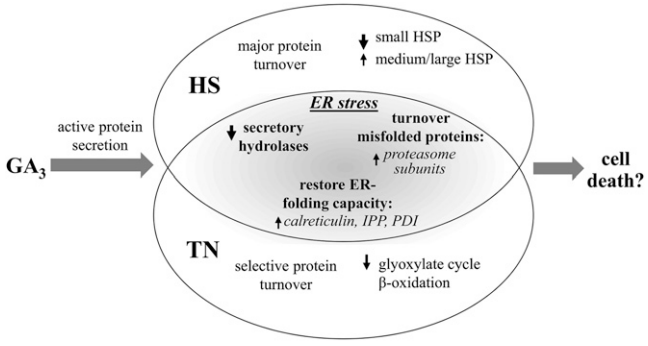

Figure 8. Summary of distinct and overlapping responses of GA_3-induced aleurone layers to HS and TN treatments. GA_3-induced aleurone layers may display early symptoms of ER stress due to the pressure on the protein secretion system and reflected by the enhanced expression of proteins induced by ER stress. IPP, Isopentenyl diphosphate isomerase.

degradation of the water-soluble protein fraction when compared with TN-treated samples, whereas the TN effect was more selective. In particular, distinct subsets of HSPs respond divergently to HS. Common components of the ER stress response induced by the TN and HS treatments include HSPs, calreticulins, enzymes of nucleotide metabolism, and isopentenyl diphosphate isomerase, and a reduction is observed in polysaccharide hydrolases and proteases in both extracellular and intracellular fractions. (3) The assignment of *N*-glycosylation sites represents a major advance in mapping the barley glycoproteome, determining the largest number of *N*-glycoproteins in this species to date. This approach provides targets for further proteomic experiments and the characterization of specific protein patterns.

In conclusion, our work emphasizes new features of the barley aleurone layer, expanding its use as a suitable model for the analysis of the plant protein secretion system and the nature of plant PTMs.

MATERIALS AND METHODS

Plant Material, Experimental Design, and Sample Preparation

Barley grains (*Hordeum vulgare* 'Himalaya', 2003 harvest), representing a pool of individuals, were purchased from Washington State University. These were used as the starting point from which replicate samples were prepared. Aleurone layers were isolated as described previously (Hynek et al., 2006). For each treatment, 100-mg aleurone layers were incubated in 2 mL of a baseline culture medium (20 mM sodium succinate and 20 mM $CaCl_2$, pH 4.2) and incubated at room temperature with continuous gentle shaking for 24 h. When 5 μM GA_3 was added to the baseline culture, samples are referred as to GA_3-induced aleurone layers. Two additional treatments were applied to aleurone layers incubated in baseline culture + 5 μM GA_3: either TN (added from a stock in methanol) or HS (40°C during the last 4 h of incubation).

Aleurone layers and incubation buffers containing the extracellular proteins from the above samples (untreated, GA_3 induced, GA_3 + HS, and GA_3 + TN) were harvested at 24 h, and samples were prepared as follows.

Intracellular Protein Fraction

Aleurone layers were washed four times with 2 mL of the baseline medium, frozen in liquid nitrogen, and stored at −80°C until use. Proteins were extracted from 100-mg aleurone layers in 1 mL of buffer (5 mM Tris-HCl and 1 mM $CaCl_2$, pH 7.5; Østergaard et al., 2002) with the protease inhibitor cocktail Complete (Roche) for 30 min in a cold room. Insoluble material was pelleted by centrifugation (10 min at 13,000 rpm, 4°C), and supernatants containing solubilized proteins were stored at −80°C until use.

Extracellular Protein Fraction

The spent incubation medium from the aleurone layers was centrifuged to remove insoluble material (5 min at 13,000 rpm, 4°C), and then supernatants containing the extracellular proteins were frozen at −80°C until use.

At least three biological replicates were used for each analysis. In each one, the whole procedure, starting from the selection of the dry seeds, was repeated.

Protein Quantification

Protein concentrations in both intracellular and extracellular protein fractions were determined using the assay of Popov et al. (1975) with bovine serum albumin as a standard.

Determination of Cell Viability and Death

The percentages of live and dead cells were determined by double staining with fluorescein diacetate (2 μg mL^{-1} in 20 mM $CaCl_2$) for 15 min, followed by N-(3-Triethylammoniumpropyl)-4-(6-(4-(diethylamino)phenyl)hexatrienyl) pyridinium dibromide (20 μM in 20 mM $CaCl_2$) for 2 min as described (Fath et al., 2001; Wu et al., 2011) with minor modifications. Aleurone layers were observed with a fluorescence microscope (Nikon Eclipse E1000; Nikon Instruments) using a 20× objective, and images were captured using a digital camera. Randomly selected fields from three different aleurone layers per treatment (biological replicates) were counted to determine the percentage of live cells.

Determination of Endogenous H_2O_2 and Lipid Peroxidation (TBARS)

The measurement of H_2O_2 in the aleurone layers was based on the peroxide-mediated oxidation of Fe^{2+}, followed by the reaction of Fe^{3+} with xylenol orange (Bellincampi et al., 2000). Absorbance values were calibrated to a standard curve generated with known concentrations of H_2O_2.

The extent of lipid peroxidation was assayed by determining the concentration of TBARS as described (Hernández and Almansa, 2002).

Four biological replicates of 20 aleurone layers per treatment were used for each analysis. Volumes of the samples and reactants were adapted for measuring the absorbance on 96-well microplates. The statistical significance of the results was analyzed according to Tukey's test ($P < 0.05$) using the XLSTAT software for Mac (Addinsoft).

Western Blotting for α-Amylase Detection

Either 5 μg of protein extracted from the aleurone layer (intracellular fraction) or proteins contained in 20 μL of the extracellular fraction was separated on 4% to 12% Bis-Tris NuPAGE gels (Invitrogen) followed by electroblotting to a nitrocellulose membrane (Hybond-ECL; Amersham, GE Healthcare) before being probed with rabbit polyclonal antibodies raised against barley α-amylase (Søgaard and Svensson, 1990). Secondary goat anti-rabbit IgG antibodies conjugated to alkaline phosphatase and 5-bromo-4-chloro-3-indolyl phosphate/nitroblue tetrazolium western-blotting reagent (Sigma Fast; Sigma-Aldrich) were used to detect binding. Three biological replicates were performed. For each one, a gel was run in parallel and stained with silver nitrate (Heukeshoven and Dernick, 1988). For analysis of the effect of HS on the extracellular α-amylase, the incubation buffer was replaced at the onset of the HS, allowing harvest of the proteins released only during the final 4 h of incubation. To enable sufficient protein to be loaded on the gel, it was necessary to concentrate these protein samples by precipitation (4 volumes of acetone at −20°C overnight).

2D Gel Electrophoresis and Staining

Gel for Mass Spectrometry Analysis

Both the secreted proteins present in 2 mL of incubation buffer and proteins from aleurone layer extractions were desalted on NAP-5 columns (GE Healthcare) following the manufacturer's instructions. Aliquots containing 140 μg of proteins were precipitated with 4 volumes of acetone and applied to 18-cm pH 3 to 10 Linear Immobilized pH Gradient (IPG) strips (Immobiline DryStrip; GE Healthcare) for first-dimension isoelectrofocusing (Shahpiri et al., 2008). The IPG strips were equilibrated and the second dimension was run on an Excel 12% to 14% gradient gel (GE Healthcare) using a Multiphor II (GE Healthcare; Shahpiri et al., 2008). Proteins were visualized by colloidal Coomassie Brilliant Blue staining (Rabilloud, 2000). At least three biological replicates were performed for each of the four treatments (four replicates were performed for GA_3 + HS [intracellular and extracellular fractions] and for the GA_3 extracellular fraction). After scanning, gel images were analyzed using the Progenesis SameSpots software (version 4.5.4325.33621; Nonlinear Dynamics). Statistical comparison of the spot intensity among the four treatments, based on one-way ANOVA ($P < 0.05$) and a fold change greater than 1.5 (calculated as the difference between the lowest and the highest mean normalized spot volumes), was verified using false discovery rate analysis ($q < 0.05$).

Gel Glycoprotein Staining and Fluorescence Visualization

Secreted proteins from GA_3 and GA_3 + 5 μg mL^{-1} TN samples (100 μg) were precipitated and run on 11-cm pH 3 to 10 Linear IPG strips as described above. The IPG strips were then trimmed to 7 cm, covering pH range 4 to 8.5, and the second-dimension SDS-PAGE (NuPAGE Novex 4-12% Bis-Tris ZOOM Gel; Invitrogen) was performed in the XCell SureLock Mini-Cell

system (Invitrogen). Gels were stained with the Pro-Q Emerald 300 Glycoprotein Gel Kit (Molecular Probes) according to the manufacturer's instructions. Three biological replicates were performed for each of the two treatments. The fluorescent spots were visualized using the UVP BioSpectrum Image System (AH Diagnostics) with transillumination at 302 nm. Images of gels were obtained using a 485- to 655-nm filter. After imaging, the gels were stained with colloidal Coomassie Brilliant Blue.

In-Gel Digestion and Protein Identification by Matrix-Assisted Laser-Desorption Ionization Time of Flight/Time of Flight

Spots of interest were excised from 2D SDS-PAGE gels and digested as described by Shevchenko et al. (1996). After soaking with trypsin (modified porcine trypsin; Promega), the gel pieces were covered with 70 μL of 10 mM $(NH_4)HCO_3$ and incubated at 37°C overnight. The supernatant containing tryptic peptides was transferred to a clean tube, and 2 μL was placed onto a matrix-assisted laser-desorption ionization anchor target. The sample was dried at room temperature and covered with 1 μL of 5 $\mu g\ \mu L^{-1}$ α-cyano-hydroxycinnamic acid in 70% (v/v) acetonitrile (ACN) and 0.1% (v/v) trifluoroacetic acid, dried again, and washed with 2 μL of 0.5% (v/v) trifluoroacetic acid. An Ultraflex II matrix-assisted laser-desorption ionization time of flight/time of flight mass spectrometer (Bruker-Daltonics) was used in positive ion reflector mode, and spectra were analyzed using FlexAnalysis software (Bruker-Daltonics). Internal calibration was carried out with trypsin autolysis products (mass-to-charge ratios 842.51 and 2,211.10).

The peptide masses and sequences obtained were matched to proteins with an in-house Mascot server (version 2.2.04), searching in the Munich Information Center for Protein Sequences barley genome database containing high-confidence gene models (ftp://ftpmips.helmholtz-muenchen.de/plants/barley/public_data/). Search parameters were as follows: allowed modifications, oxidation of Met (variable) and carbamidomethylation of Cys (static); monoisotopic mass tolerance, 40 ppm; allowed missed cleavages, one.

Positive protein identifications were considered when one of the following requirements was met: three independent peptides, where one of them was confirmed by MS/MS fragment ion fingerprinting; or two independent peptides, both confirmed by MS/MS. For details, see Supplemental Tables S1 to S3.

Identification of *N*-Glycosylated Proteins from Complex Samples and Assignment of Their Glycosylation Sites

In-Solution Digestion and HILIC

Protein samples from both intracellular and extracellular fractions were digested in solution as described (Hägglund et al., 2004) and applied to microcolumns containing a combination of Zwitterion-HILIC resin and cotton. A small piece of cotton wool (approximately 200 μg) taken from a cotton wool pad was pushed into a 20-μL GELoader tip (Eppendorf), and ZIC-HILIC resin (Sequant; particle size, 10 μm) was packed on top of the cotton wool. The microcolumns were equilibrated with 40 μL of 80% (v/v) ACN and 0.5% (v/v) formic acid (FA). In-solution trypsin-digested protein samples (20 μg) were dried (SPD 1010 Speed Vac; Thermo Scientific), redissolved in 40 μL of 80% (v/v) ACN and 0.5% (v/v) FA, and applied onto the equilibrated HILIC microcolumns. The column was washed twice with 80% (v/v) ACN and 0.5% (v/v) FA, followed by elution of bound peptides in 0.5% (v/v) FA.

Endoglycosidase Digestion and Protein Identification by Q-Exactive LC-MS/MS

Deglycosylation of the eluted peptides was performed in 100 mM ammonium acetate prepared in $H_2{}^{18}O$-water for 24 h at 37°C with 0.1 milliunit of *N*-glycosidase A (PNGase A; Roche). To minimize ^{18}O isotope labeling at peptide C termini, the deglycosylated samples were dried, redissolved in 100 mM ammonium acetate prepared in $H_2{}^{16}O$-water, and incubated for 24 h at 37°C in the presence of 0.2 μg of sequencing-grade modified trypsin (Promega). The peptides were desalted on a StageTip C18 reverse-phase column (Thermo Scientific) and separated on an EASY-Spray column (Pepmap 3 μm, C18 15 cm × 75 μm) coupled online to a Q-Exactive Orbitrap (Thermo Scientific). The separation was performed using a flow rate of 300 nL min^{-1} and a gradient of solvents A (0.1% FA) and B (80% ACN and 0.1% FA) as follows: 5% to 40% B for 40 min; 40% to 100% B for 5 min; 100% B for 10 min. The LC-mass spectrometry data were processed using Proteome Discoverer software (version 1.3; Thermo Scientific) and then searched using Mascot (version 2.2.04) against the Munich Information Center for Protein Sequences barley genome database (as above). Mass spectrometry and MS/MS accuracy were 10 ppm and 20 milli mass units (mmu), respectively. In addition to oxidation of Met, variable modifications were set to include deamidation of Asn or Gln with incorporation of ^{16}O (Asn/Gln + 0.98 D), ^{18}O (Asn/Gln + 2.99 D), and the incorporation of one or two ^{18}O atoms at the peptide C terminus. Carbamidomethyl Cys was set as a fixed modification. In order to be accepted as a glycopeptide, the deamidated residue containing ^{18}O atoms had to be situated within a consensus sequence for *N*-glycoslation (NXS/T).

Supplemental Data

The following materials are available in the online version of this article.

Supplemental Table S1. Identification of candidate glycoproteins by Pro-Q Emerald staining in extracellular fractions of GA_3-induced aleurone layers.

Supplemental Table S2. Proteins identified in extracellular fractions of 24-h incubated aleurone layers.

Supplemental Table S3. Proteins identified in intracellular water-soluble fractions of 24-h incubated aleurone layers.

Supplemental Table S4. Identification of *N*-glycosylated proteins from complex samples and assignment of their glycosylation sites.

ACKNOWLEDGMENTS

We thank Birgit Andersen for excellent laboratory assistance and mass spectrometry analysis, Martin Kogle for help with microscopy experiments, and Susanne Jacobsen for valuable discussion and support.

Received November 26, 2013; accepted December 11, 2013; published December 13, 2013.

LITERATURE CITED

Agrawal GK, Jwa NS, Lebrun MH, Job D, Rakwal R (2010) Plant secretome: unlocking secrets of the secreted proteins. Proteomics **10:** 799–827

Alexandersson E, Ali A, Resjö S, Andreasson E (2013) Plant secretome proteomics. Front Plant Sci **4:** 9

Apweiler R, Hermjakob H, Sharon N (1999) On the frequency of protein glycosylation, as deduced from analysis of the SWISS-PROT database. Biochim Biophys Acta **1473:** 4–8

Bailly C (2004) Active oxygen species and antioxidants in seed biology. Seed Sci Res **14:** 93–107

Bailly C, El-Maarouf-Bouteau H, Corbineau F (2008) From intracellular signaling networks to cell death: the dual role of reactive oxygen species in seed physiology. C R Biol **331:** 806–814

Bak-Jensen KS, Laugesen S, Ostergaard O, Finnie C, Roepstorff P, Svensson B (2007) Spatio-temporal profiling and degradation of α-amylase isozymes during barley seed germination. FEBS J **274:** 2552–2565

Barba-Espín G, Diaz-Vivancos P, Job D, Belghazi M, Job C, Hernández JA (2011) Understanding the role of H_2O_2 during pea seed germination: a combined proteomic and hormone profiling approach. Plant Cell Environ **34:** 1907–1919

Belanger FC, Brodl MR, Ho TH (1986) Heat shock causes destabilization of specific mRNAs and destruction of endoplasmic reticulum in barley aleurone cells. Proc Natl Acad Sci USA **83:** 1354–1358

Bellincampi D, Dipierro N, Salvi G, Cervone F, De Lorenzo G (2000) Extracellular H_2O_2 induced by oligogalacturonides is not involved in the inhibition of the auxin-regulated *rolB* gene expression in tobacco leaf explants. Plant Physiol **122:** 1379–1385

Bethke P, Schuurink R, Jones RL (1997) Hormonal signalling in cereal aleurone. J Exp Bot **48:** 1337–1356

Bethke PC, Jones RL (2001) Cell death of barley aleurone protoplasts is mediated by reactive oxygen species. Plant J **25:** 19–29

Bond U, Schlesinger MJ (1986) The chicken ubiquitin gene contains a heat shock promoter and expresses an unstable mRNA in heat-shocked cells. Mol Cell Biol **6:** 4602–4610

Bønsager BC, Finnie C, Roepstorff P, Svensson B (2007) Spatio-temporal changes in germination and radical elongation of barley seeds tracked by proteome analysis of dissected embryo, aleurone layer, and endosperm tissues. Proteomics **7:** 4528–4540

Brodl MR, Ho THD (1991) Heat shock causes selective destabilization of secretory protein mRNAs in barley aleurone cells. Plant Physiol **96:** 1048–1052

Bunkenborg J, Pilch BJ, Podtelejnikov AV, Wiśniewski JR (2004) Screening for *N*-glycosylated proteins by liquid chromatography mass spectrometry. Proteomics **4:** 454–465

Bush DS, Cornejo MJ, Huang CN, Jones RL (1986) Ca-stimulated secretion of α-amylase during development in barley aleurone protoplasts. Plant Physiol **82:** 566–574

Chrispeels MJ, Varner JE (1967) Gibberellic acid-enhanced synthesis and release of α-amylase and ribonuclease by isolated barley and aleurone layers. Plant Physiol **42:** 398–406

Craig EA, Weissman JS, Horwich AL (1994) Heat shock proteins and molecular chaperones: mediators of protein conformation and turnover in the cell. Cell **78:** 365–372

Denecke J, Carlsson LE, Vidal S, Höglund AS, Ek B, van Zeijl MJ, Sinjorgo KM, Palva ET (1995) The tobacco homolog of mammalian calreticulin is present in protein complexes *in vivo*. Plant Cell **7:** 391–406

De Wilde K, De Buck S, Vanneste K, Depicker A (2013) Recombinant antibody production in Arabidopsis seeds triggers an unfolded protein response. Plant Physiol **161:** 1021–1033

Doig RI, Colborne AJ, Morris G, Laidman DL (1975) The induction of glyoxysomal enzyme activities in the aleurone cells of germinating wheat. J Exp Bot **26:** 387–398

Eastmond PJ, Jones RL (2005) Hormonal regulation of gluconeogenesis in cereal aleurone is strongly cultivar-dependent and gibberellin action involves SLENDER1 but not GAMYB. Plant J **44:** 483–493

Erlendsson LS, Muench MO, Hellman U, Hrafnkelsdóttir SM, Jonsson A, Balmer Y, Mäntylä E, Örvar BL (2010) Barley as a green factory for the production of functional Flt3 ligand. Biotechnol J **5:** 163–171

Fath A, Bethke PC, Jones RL (2001) Enzymes that scavenge reactive oxygen species are down-regulated prior to gibberellic acid-induced programmed cell death in barley aleurone. Plant Physiol **126:** 156–166

Finnie C, Andersen B, Shahpiri A, Svensson B (2011) Proteomes of the barley aleurone layer: a model system for plant signalling and protein secretion. Proteomics **11:** 1595–1605

Finnie C, Svensson B (2003) Feasibility study of a tissue-specific approach to barley proteome analysis: aleurone layer, endosperm, embryo and single seeds. J Cereal Sci **38:** 217–227

Fitchette AC, Dinh OT, Faye L, Bardor M (2007) Plant proteomics and glycosylation. Methods Mol Biol **355:** 317–342

Gardai SJ, McPhillips KA, Frasch SC, Janssen WJ, Starefeldt A, Murphy-Ullrich JE, Bratton DL, Oldenborg PA, Michalak M, Henson PM (2005) Cell-surface calreticulin initiates clearance of viable or apoptotic cells through trans-activation of LRP on the phagocyte. Cell **123:** 321–334

Gold LI, Eggleton P, Sweetwyne MT, Van Duyn LB, Greives MR, Naylor SM, Michalak M, Murphy-Ullrich JE (2010) Calreticulin: non-endoplasmic reticulum functions in physiology and disease. FASEB J **24:** 665–683

Hägglund P, Bunkenborg J, Elortza F, Jensen ON, Roepstorff P (2004) A new strategy for identification of *N*-glycosylated proteins and unambiguous assignment of their glycosylation sites using HILIC enrichment and partial deglycosylation. J Proteome Res **3:** 556–566

Hägglund P, Bunkenborg J, Yang F, Harder LM, Finnie C, Svensson B (2010) Identification of thioredoxin target disulfides in proteins released from barley aleurone layers. J Proteomics **73:** 1133–1136

Hernández JA, Almansa MS (2002) Short-term effects of salt stress on antioxidant systems and leaf water relations of pea leaves. Physiol Plant **115:** 251–257

Heukeshoven J, Dernick R (1988) Improved silver staining procedure for fast staining in PhastSystem development unit. I. Staining of sodium dodecyl sulfate gels. Electrophoresis **9:** 28–32

Hynek R, Svensson B, Jensen ON, Barkholt V, Finnie C (2006) Enrichment and identification of integral membrane proteins from barley aleurone layers by reversed-phase chromatography, SDS-PAGE, and LC-MS/MS. J Proteome Res **5:** 3105–3113

Ishibashi Y, Tawaratsumida T, Kondo K, Kasa S, Sakamoto M, Aoki N, Zheng SH, Yuasa T, Iwaya-Inoue M (2012) Reactive oxygen species are involved in gibberellin/abscisic acid signaling in barley aleurone cells. Plant Physiol **158:** 1705–1714

Jerkovic A, Kriegel AM, Bradner JR, Atwell BJ, Roberts TH, Willows RD (2010) Strategic distribution of protective proteins within bran layers of wheat protects the nutrient-rich endosperm. Plant Physiol **152:** 1459–1470

Johnston MK, Jacob NP, Brodl MR (2007) Heat shock-induced changes in lipid and protein metabolism in the endoplasmic reticulum of barley aleurone layers. Plant Cell Physiol **48:** 31–41

Jones MB, Rosenberg JN, Betenbaugh MJ, Krag SS (2009) Structure and synthesis of polyisoprenoids used in *N*-glycosylation across the three domains of life. Biochim Biophys Acta **1790:** 485–494

Jones RL, Jacobsen JV (1991) Regulation of synthesis and transport of secreted proteins in cereal aleurone. Int Rev Cytol **126:** 49–88

Kamauchi S, Nakatani H, Nakano C, Urade R (2005) Gene expression in response to endoplasmic reticulum stress in Arabidopsis thaliana. FEBS J **272:** 3461–3476

Kim SY, Paeng SK, Nawkar GM, Maibam P, Lee ES, Kim KS, Lee DH, Park DJ, Kang SB, Kim MR, et al (2011) The 1-Cys peroxiredoxin, a regulator of seed dormancy, functions as a molecular chaperone under oxidative stress conditions. Plant Sci **181:** 119–124

Koehler SM, Ho TH (1990) Hormonal regulation, processing, and secretion of cysteine proteinases in barley aleurone layers. Plant Cell **2:** 769–783

Laubin B, Lullien-Pellerin V, Nadaud I, Gaillard-Martiniec B, Chambond C, Branlard G (2008) Isolation of the wheat aleurone layer for 2D electrophoresis and proteomics analysis. J Cereal Sci **48:** 709–714

Martínez IM, Chrispeels MJ (2003) Genomic analysis of the unfolded protein response in *Arabidopsis* shows its connection to important cellular processes. Plant Cell **15:** 561–576

Martinez M, Diaz I (2008) The origin and evolution of plant cystatins and their target cysteine proteinases indicate a complex functional relationship. BMC Evol Biol **8:** 198

Maya-Ampudia V, Bernal-Lugo I (2006) Redox-sensitive target detection in gibberellic acid-induced barley aleurone layer. Free Radic Biol Med **40:** 1362–1368

Melo-Braga MN, Verano-Braga T, León IR, Antonacci D, Nogueira FC, Thelen JJ, Larsen MR, Palmisano G (2012) Modulation of protein phosphorylation, N-glycosylation and Lys-acetylation in grape (*Vitis vinifera*) mesocarp and exocarp owing to *Lobesia botrana* infection. Mol Cell Proteomics **11:** 945–956

Meziani S, Nadaud I, Gaillard-Martinie B, Chambon C, Benali M, Branlard G (2012) Proteomic analysis of the mature kernel aleurone layer in common and durum wheat. **55:** J Cereal Sci 323–330

Minic Z, Jamet E, Négroni L, Arsene der Garabedian P, Zivy M, Jouanin L (2007) A sub-proteome of Arabidopsis thaliana mature stems trapped on concanavalin A is enriched in cell wall glycoside hydrolases. J Exp Bot **58:** 2503–2512

Moreno AA, Mukhtar MS, Blanco F, Boatwright JL, Moreno I, Jordan MR, Chen Y, Brandizzi F, Dong X, Orellana A, et al (2012) *IRE1/bZIP60*-mediated unfolded protein response plays distinct roles in plant immunity and abiotic stress responses. PLoS ONE **7:** e31944

Nagashima Y, Mishiba K, Suzuki E, Shimada Y, Iwata Y, Koizumi N (2011) Arabidopsis IRE1 catalyses unconventional splicing of bZIP60 mRNA to produce the active transcription factor. Sci Rep **1:** 29–38

Noh SJ, Kwon CS, Oh DH, Moon JS, Chung WI (2003) Expression of an evolutionarily distinct novel BiP gene during the unfolded protein response in *Arabidopsis thaliana*. Gene **311:** 81–91

Nothaft H, Szymanski CM (2010) Protein glycosylation in bacteria: sweeter than ever. Nat Rev Microbiol **8:** 765–778

Østergaard O, Melchior S, Roepstorff P, Svensson B (2002) Initial proteome analysis of mature barley seeds and malt. Proteomics **2:** 733–739

Palmisano G, Antonacci D, Larsen MR (2010) Glycoproteomic profile in wine: a 'sweet' molecular renaissance. J Proteome Res **9:** 6148–6159

Popov N, Schmitt M, Schulzeck S, Matthies H (1975) [Reliable micromethod for determination of the protein content in tissue homogenates]. Acta Biol Med Ger **34:** 1441–1446

Pulido P, Domínguez F, Cejudo FJ (2009) A hydrogen peroxide detoxification system in the nucleus of wheat seed cells: protection or signaling role? Plant Signal Behav **4:** 23–25

Rabilloud T (2000) Detecting proteins separated by 2-D gel electrophoresis. Anal Chem **72:** 48A–55A

Reis PA, Rosado GL, Silva LA, Oliveira LC, Oliveira LB, Costa MD, Alvim FC, Fontes EP (2011) The binding protein BiP attenuates stress-induced cell death in soybean via modulation of the N-rich protein-mediated signaling pathway. Plant Physiol **157:** 1853–1865

Shahpiri A, Svensson B, Finnie C (2008) The NADPH-dependent thioredoxin reductase/thioredoxin system in germinating barley seeds: gene expression, protein profiles, and interactions between isoforms of thioredoxin *h* and thioredoxin reductase. Plant Physiol **146:** 789–799

Shaw AE, Brodl MR (2003) Heat shock response of warm-incubated barley aleurone layers. Am J Bot **90:** 40–48

Shevchenko A, Wilm M, Vorm O, Mann M (1996) Mass spectrometric sequencing of proteins silver-stained polyacrylamide gels. Anal Chem **68:** 850–858

Søgaard M, Svensson B (1990) Expression of cDNAs encoding barley alpha-amylase 1 and 2 in yeast and characterization of the secreted proteins. Gene **94:** 173–179

Spiess C, Beil A, Ehrmann M (1999) A temperature-dependent switch from chaperone to protease in a widely conserved heat shock protein. Cell **97:** 339–347

Stacy RAP, Nordeng TW, Culiáñez-Macià FA, Aalen RB (1999) The dormancy-related peroxiredoxin anti-oxidant, PER1, is localized to the nucleus of barley embryo and aleurone cells. Plant J **19:** 1–8

Tasleem-Tahir A, Nadaud I, Girousse C, Martre P, Marion D, Branlard G (2011) Proteomic analysis of peripheral layers during wheat (*Triticum aestivum* L.) grain development. Proteomics **11:** 371–379

Terashima M, Kubo A, Suzawa M, Itoh Y, Katoh S (1994) The roles of the N-linked carbohydrate chain of rice α-amylase in thermostability and enzyme kinetics. Eur J Biochem **226:** 249–254

Thannhauser TW, Shen M, Sherwood R, Howe K, Fish T, Yang Y, Chen W, Zhang S (2013) A workflow for large-scale empirical identification of cell wall N-linked glycoproteins of tomato (*Solanum lycopersicum*) fruit by tandem mass spectrometry. Electrophoresis **34:** 2417–2431

Travers KJ, Patil CK, Wodicka L, Lockhart DJ, Weissman JS, Walter P (2000) Functional and genomic analyses reveal an essential coordination between the unfolded protein response and ER-associated degradation. Cell **101:** 249–258

Wang W, Vinocur B, Shoseyov O, Altman A (2004) Role of plant heat-shock proteins and molecular chaperones in the abiotic stress response. Trends Plant Sci **9:** 244–252

Witzel K, Weidner A, Surabhi GK, Varshney RK, Kunze G, Buck-Sorlin GH, Börner A, Mock HP (2010) Comparative analysis of the grain proteome fraction in barley genotypes with contrasting salinity tolerance during germination. Plant Cell Environ **33:** 211–222

Wollscheid B, Bausch-Fluck D, Henderson C, O'Brien R, Bibel M, Schiess R, Aebersold R, Watts JD (2009) Mass-spectrometric identification and relative quantification of *N*-linked cell surface glycoproteins. Nat Biotechnol **27:** 378–386

Wu C, Ma CQ, Pan Y, Gong SL, Zhao CX, Chen SX, Li HY (2013) Sugar beet M14 glyoxalase I gene can enhance plant tolerance to abiotic stresses. J Plant Res **126:** 415–425

Wu M, Huang J, Xu S, Ling T, Xie Y, Shen W (2011) Haem oxygenase delays programmed cell death in wheat aleurone layers by modulation of hydrogen peroxide metabolism. J Exp Bot **62:** 235–248

Ye C, Dickman MB, Whitham SA, Payton M, Verchot J (2011) The unfolded protein response is triggered by a plant viral movement protein. Plant Physiol **156:** 741–755

Zhang N, Jones BL (1995) Characterization of germinated barley endoproteolytic enzymes by two dimensional gel electrophoresis. J Cereal Sci **21:** 145–153

Zhang S, Sherwood RW, Yang Y, Fish T, Chen W, McCardle JA, Jones RM, Yusibov V, May ER, Rose JK, et al (2012) Comparative characterization of the glycosylation profiles of an influenza hemagglutinin produced in plant and insect hosts. Proteomics **12:** 1269–1288

Zielinska DF, Gnad F, Wiśniewski JR, Mann M (2010) Precision mapping of an in vivo N-glycoproteome reveals rigid topological and sequence constraints. Cell **141:** 897–907

Zrenner R, Stitt M, Sonnewald U, Boldt R (2006) Pyrimidine and purine biosynthesis and degradation in plants. Annu Rev Plant Biol **57:** 805–836